

13. B. Schrank *et al.*, *Proc. Natl. Acad. Sci. U.S.A.* **94**, 9920–9925 (1997).
14. S. Paushkin, A. K. Gubitz, S. Massenet, G. Dreyfuss, *Curr. Opin. Cell Biol.* **14**, 305–312 (2002).
15. A. H. Burghes, C. E. Beattie, *Nat. Rev. Neurosci.* **10**, 597–609 (2009).
16. M. D. Mailman *et al.*, *Genet. Med.* **4**, 20–26 (2002).
17. T. O. Crawford *et al.*, *PLoS ONE* **7**, e33572 (2012).
18. B. Wirth *et al.*, *Hum. Genet.* **119**, 422–428 (2006).
19. M. Feldkötter, V. Schwarzer, R. Wirth, T. F. Wienker, B. Wirth, *Am. J. Hum. Genet.* **70**, 358–368 (2002).
20. E. Arkblad, M. Tulinius, A. K. Kroksmark, M. Henriksen, N. Darin, *Acta Paediatr.* **98**, 865–872 (2009).
21. S. J. Kolb *et al.*, *BMC Neurol.* **6**, 6 (2006).
22. K. Takata, T. Shimizu, S. Iwai, R. D. Wood, *J. Biol. Chem.* **281**, 23445–23455 (2006).
23. G. L. Moldovan *et al.*, *Mol. Cell. Biol.* **30**, 1088–1096 (2010).
24. L. Zietlow, L. A. Smith, M. Bessho, T. Bessho, *Biochemistry* **48**, 11817–11824 (2009).
25. A. M. Burroughs *et al.*, *Genome Res.* **20**, 1398–1410 (2010).
26. Z. S. Kai, A. E. Pasquinelli, *Nat. Struct. Mol. Biol.* **17**, 5–10 (2010).
27. T. Katoh *et al.*, *Genes Dev.* **23**, 433–438 (2009).
28. E. R. Kinjo *et al.*, *Exp. Neurol.* **248**, 546–558 (2013).
29. N. N. Singh, R. N. Singh, E. J. Androphy, *Nucleic Acids Res.* **35**, 371–389 (2007).
30. C. L. Lorson, E. J. Androphy, *Hum. Mol. Genet.* **9**, 259–265 (2000).
31. L. Cartegni, M. L. Hastings, J. A. Calarco, E. de Stanchina, A. R. Krainer, *Am. J. Hum. Genet.* **78**, 63–77 (2006).
32. N. N. Singh, R. N. Singh, *RNA Biol.* **8**, 600–606 (2011).
33. N. N. Singh, E. J. Androphy, R. N. Singh, *Crit. Rev. Eukaryot. Gene Expr.* **14**, 271–285 (2004).
34. M. Osborne *et al.*, *Hum. Mol. Genet.* **21**, 4431–4447 (2012).
35. T. T. Le *et al.*, *Hum. Mol. Genet.* **14**, 845–857 (2005).
36. J. Seo, M. D. Howell, N. N. Singh, R. N. Singh, *Biochim. Biophys. Acta* **1832**, 2180–2190 (2013).
37. K. O'Brien, A. J. Matlin, A. M. Lowell, M. J. Moore, *J. Biol. Chem.* **283**, 33147–33154 (2008).
38. A. N. Kuhn, M. A. van Santen, A. Schwienhorst, H. Urlaub, R. Lührmann, *RNA* **15**, 153–175 (2009).
39. D. Kaida *et al.*, *Nat. Chem. Biol.* **3**, 576–583 (2007).
40. M. Hasegawa *et al.*, *ACS Chem. Biol.* **6**, 229–233 (2011).
41. M. G. Berg *et al.*, *Mol. Cell. Biol.* **32**, 1271–1283 (2012).
42. J. G. Chang *et al.*, *PLoS ONE* **6**, e18643 (2011).
43. I. Younis *et al.*, *Mol. Cell. Biol.* **30**, 1718–1728 (2010).
44. N. N. Singh *et al.*, *Nucleic Acids Res.* **41**, 8144–8165 (2013).
45. M. A. Passini *et al.*, *Sci. Transl. Med.* **3**, 72ra18 (2011).
46. Y. Hua *et al.*, *Nature* **478**, 123–126 (2011).
47. K. Sahashi *et al.*, *EMBO Mol. Med.* **5**, 1586–1601 (2013).
48. F. Degorce *et al.*, *Curr. Chem. Genomics* **3**, 22–32 (2009).

ACKNOWLEDGMENTS

We thank O. Khwaja, C. Czech, T. Kremer, L. Müller, W. Muster, S. Kirchner, L. Green, E. Pinard, J. Kazenwadel, C. Horn, O. Spleiss, C. Sarry, P. Kueng, F. Knoflach, L. Himmelein, F. Birzele, K. von Herrmann, A. Mollin, J. Hedrick, M. Dumble, I. Huq, P. Martin, D. Mankoff, S. Jung, J. Crona, M. Haley, T. Yang, S. Choi, S. Hwang, M. Dali, W. Lennox, S. Yeh, J. Yang, J. Petruska, J. Breslin, J. Baird, B. Scharf, T. Tripodi, G. Ryan, J. Tivade, J. Du, D. Minn, C. Romfo, and C. Trotta for help and support with this project. This work was supported by grants from the SMA Foundation and the Harvard Stem Cell Institute. F. Hoffmann-La Roche and PTC Therapeutics have filed three patent applications entitled “Compounds for Treating Spinal Muscular Atrophy” (WO2013/101974 A1, WO2013/112788 A1, and WO2013/119916 A2).

SUPPLEMENTARY MATERIALS

www.sciencemag.org/content/345/6197/688/suppl/DC1
Materials and Methods
Figs. S1 to S9
Tables S1 to S4
References (49–56)
Movies S1 to S3

23 December 2013; accepted 24 June 2014
10.1126/science.1250127

LIPID CELL BIOLOGY

Polyunsaturated phospholipids facilitate membrane deformation and fission by endocytic proteins

Mathieu Pinot,^{1,2} Stefano Vanni,¹ Sophie Pagnotta,³ Sandra Lacas-Gervais,³ Laurie-Anne Payet,⁴ Thierry Ferreira,⁴ Romain Gautier,¹ Bruno Goud,² Bruno Antony,^{1*} Hélène Barelli¹

Phospholipids (PLs) with polyunsaturated acyl chains are extremely abundant in a few specialized cellular organelles such as synaptic vesicles and photoreceptor discs, but their effect on membrane properties is poorly understood. Here, we found that polyunsaturated PLs increased the ability of dynamin and endophilin to deform and vesiculate synthetic membranes. When cells incorporated polyunsaturated fatty acids into PLs, the plasma membrane became more amenable to deformation by a pulling force and the rate of endocytosis was accelerated, in particular, under conditions in which cholesterol was limiting. Molecular dynamics simulations and biochemical measurements indicated that polyunsaturated PLs adapted their conformation to membrane curvature. Thus, by reducing the energetic cost of membrane bending and fission, polyunsaturated PLs may help to support rapid endocytosis.

Most cellular membranes contain phospholipids (PLs) with saturated and mono-unsaturated acyl chains. However, in a few specialized organelles, such as synaptic vesicles, up to 80% of PLs contain at least one polyunsaturated acyl chain (1, 2). Such high levels suggest that polyunsaturated lipids might endow membranes with specific physicochemical properties.

In photoreceptor discs, which are perfectly flat, polyunsaturated PLs facilitate the conformational change of rhodopsin (3). The influence of polyunsaturated PLs on protein machineries that act on curved membranes is unclear. Nevertheless, exogenous treatment of neurons with polyunsaturated fatty acids facilitates SNARE (soluble N-ethylmaleimide-sensitive factor attachment protein receptor) assembly (4) and the recycling of synaptic vesicles (5, 6). Furthermore, polyunsaturated PLs make pure lipid bilayers more flexible (7).

We studied the effect of polyunsaturated PLs on the activity of the guanosine triphosphatase (GTPase) dynamin and the banana-shaped protein endophilin, which cooperate in membrane fission by assembling into spirals around the neck of membrane buds (8, 9). We used liposomes or giant unilamellar vesicles (GUVs) with a fixed composition in terms of PL polar head groups and varied the ratio between mono and polyunsaturated PLs (tables S1 and S2; also see supplementary materials and methods). We chose

C16:0-C18:1 and C18:0-C22:6 PLs (Fig. 1A) because they are the most abundant of each PL class.

Dynamin hydrolyzed guanosine triphosphate (GTP) 7.5 times faster on large liposomes containing polyunsaturated PLs compared with monounsaturated PLs (Fig. 1B and fig. S1A). Moreover, polyunsaturated PLs eliminated the sharp response of dynamin to membrane curvature (Fig. 1C and fig. S1B) (10). Because GTP hydrolysis occurs through contacts between dynamin molecules within the assembled spiral (11), these results suggest that polyunsaturated PLs facilitate dynamin self-assembly on flat membranes.

Using electron microscopy, we analyzed our liposomes incubated with dynamin, endophilin, and GTP, a mixture optimal for membrane fission (12). Before incubation, the liposomes displayed a similar size distribution (radius $R = 30$ to 200 nm) (Fig. 1, D and E). After incubation, polyunsaturated liposomes were consumed into small vesicles ($R \approx 20$ nm), whereas monounsaturated liposomes appeared unchanged (Fig. 1, D and E, and fig. S2, A and D). When GTP hydrolysis was blocked, characteristic endophilin-dynamin spirals (8, 9) formed on polyunsaturated liposomes, but not on monounsaturated liposomes (Fig. 1D and fig. S2, B, C, and E). Thus, polyunsaturated membranes are sensitized to the mechanical activities of the endophilin-dynamin complex.

Adhesion of liposomes to the electron microscopy grid can lead to an overestimate of authentic fission owing to membrane breakage on the stiff support (13). To overcome this caveat, we used fission assays based on visualization of model membranes by fluorescence microscopy. First, we incubated GUVs with dynamin, endophilin, and GTP and monitored the GUV diameter over time (12). GUVs containing polyunsaturated PLs showed a 14 to 30% decrease in size within 1 hour, suggesting consumption by membrane fission, whereas GUVs made of monounsaturated

¹Institut de Pharmacologie Moléculaire et Cellulaire, Université Nice Sophia Antipolis and CNRS, 06560 Valbonne, France. ²Unité Mixte de Recherche 144, Institut Curie and CNRS, F-75248 Paris, France. ³Centre Commun de Microscopie Appliquée, Université Nice Sophia Antipolis, Parc Valrose, 06000 Nice, France. ⁴Signalisation et Transports Ioniques Membranaires, Université de Poitiers and CNRS, Poitiers, France.

*Corresponding author. E-mail: antony@ipmc.cnrs.fr

PLs remained unchanged (fig. S3 and movie S1). Second, we added dynamin, endophilin, and GTP to preformed membrane tubes to observe fission events directly (14). Again, the difference between mono and polyunsaturated membranes was notable: 95% of the tubes ($n = 96$) containing polyunsaturated PLs underwent fission, as compared with 4% of the tubes ($n = 52$) made of monounsaturated PLs (Fig. 1, F and G, and movie S2).

Next, we tested the effects of polyunsaturated PLs on the mechanical properties of the plasma membrane (PM), on which endophilin and dynamin act. We cultured epithelial cells (RPE1) with defined fatty acids and used optical tweezers to pull tubes from the PM. Lipid analysis showed that the cells incorporated C22:6 into cellular PLs within a few hours (Fig. 2A and fig. S4). To facilitate mechanical manipulation, we cultured cells on L-shaped micropatterns on which they adopted a triangular shape (Fig. 2B). We pulled tubes from the cell hypotenuse and measured the pulling force (F) and the tube apparent ra-

dius (R) (Fig. 2, B to D, and fig. S5, A to C). Cells incubated with C22:6 showed a 1.8-fold decrease in F and a 2.5-fold decrease in R within 1 hour, whereas cells incubated with C18:1 showed no significant changes (Fig. 2, E and F). Because F and R are related to the bending rigidity (κ) and membrane tension (σ) by $\kappa = \frac{FR}{2\pi}$ and $\sigma = \frac{F}{4\pi R}$ (15), the parallel decrease in F and R indicates that C22:6 incorporation decreased the bending rigidity by \approx fourfold (Fig. 2G), as compared with a twofold decrease for GUVs containing 30 mole percent (mol %) polyunsaturated PLs (Fig. 2H), but did not affect membrane tension, which depended on interactions with the actin cytoskeleton (fig. S5, D to F).

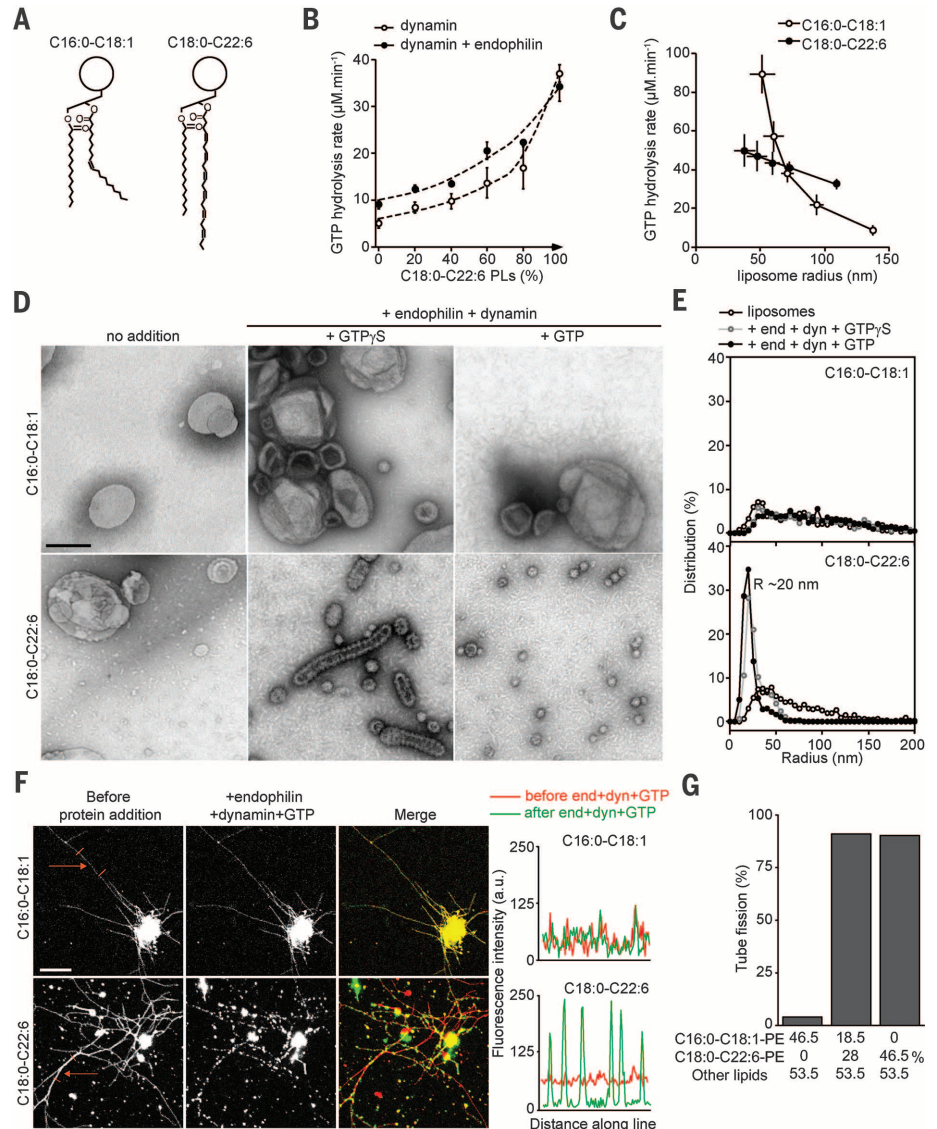
By making the PM more flexible, polyunsaturated PLs might facilitate endocytic events—in particular, clathrin-mediated endocytosis—as suggested by the effect of C18:3, the precursor of C22:6, on model dopaminergic cells (16). Cells fed with C22:6 displayed a 1.5-fold higher transferrin (Tfn) uptake than C18:1-fed cells (Fig. 3, A and B). Because cholesterol alleviates membrane

deformation stress by flip-flopping between bilayer leaflets (17–19), we depleted cholesterol from the PM using methyl- β -cyclodextrin (MCD) to better isolate the contribution of polyunsaturated PLs. MCD completely inhibited Tfn uptake in C18:1-fed cells, but not in C22:6-fed cells (Fig. 3, A and B). Moreover, when we overexpressed endophilin, Tfn uptake under low-cholesterol conditions was nine times more efficient in C22:6 than in C18:1-treated cells (Fig. 3, A and C). Dyngo 4a, a specific dynamin inhibitor (20), inhibited this endophilin-stimulated endocytosis (fig. S6). Thus, polyunsaturated PLs can facilitate endocytic events that are under the dual control of endophilin and dynamin.

Polyunsaturated acyl chains reside closer to the bilayer-water interface than other acyl chains, owing to the ability of polyunsaturated acyl chains to adopt bent conformations (21, 22). How this feature varies with curvature should give insight into the benefit of polyunsaturated PLs for membrane deformation. However, given the difficulties in addressing lipid conformation in membranes

Fig. 1. Polyunsaturated PLs facilitate membrane fission by endophilin and dynamin.

(A) Schemes of monounsaturated and polyunsaturated PLs used in this study. (B) GTPase rate of dynamin (0.3 μ M) \pm endophilin (1 μ M) with large liposomes (400-nm extrusion) containing increasing ratio of polyunsaturated versus monounsaturated PLs. Data are mean \pm SD from three independent experiments. (C) GTPase rate of dynamin (0.3 μ M) with liposomes obtained by extrusion through 400-, 200-, 100-, 50-, or 30-nm filters and containing monounsaturated or polyunsaturated PLs. Liposome radius was assessed by dynamic light scattering. Data are mean \pm SD from three independent experiments. (D) Electron micrographs of C16:0-C18:1 or C18:0-C22:6 liposomes (400-nm extrusion) before or after incubation with dynamin (0.5 μ M), endophilin (1 μ M), and GTP or GTP γ S (500 μ M). Scale bar, 200 nm. (E) Size distributions of the membrane profiles, as determined from two independent experiments similar to that shown in (D). For each condition, 500 to 1100 profiles were analyzed. (F) Tube fission assay. Membrane tubes containing C16:0-C18:1 phosphatidylethanolamine (PE) or C18:0-C22:6 PE (28 mol %) were visualized before and 10 to 20 s after the addition of endophilin (1 μ M), dynamin (0.5 μ M), and GTP (500 μ M). The tube networks are shown in arbitrary colors. Red, before; green, after protein addition. The profiles show the lipid fluorescence along the tubes indicated by arrows. Scale bar, 10 μ m. a.u., arbitrary units. (G) Quantification of tube fission. For each condition, 52 to 96 tubes from two to three independent experiments were examined. See tables S1 and S2 for the liposome composition.



of complex geometries, we performed coarse-grain molecular dynamics (MD) simulations.

We mimicked the process of membrane deformation by applying a pulling force to a phosphatidylcholine (PC) bilayer (23). The resulting membrane tube was thinner when the bilayer contained polyunsaturated PLs compared with monounsaturated ones, suggesting a decrease in bending rigidity (Fig. 4B and movie S3).

Estimating the bending modulus from buckled bilayers (fig. S7A) or from the undulations of flat bilayers (fig. S7B) indicated a twofold decrease in κ . Next, we increased the pulling force and observed that the tube frequently underwent fission (Fig. 4A and movie S3). Computing the force and tube radius immediately before fission indicated that polyunsaturated PLs lowered the force threshold (Fig. 4B and fig. S7C) but did not

change the critical radius for fission ($R_c \approx 4$ nm) (Fig. 4B). Thus, the coarse-grain simulation approach recapitulates the properties of polyunsaturated membranes: they are more prone to deformation and fission.

We therefore used MD to analyze the conformation of the PL acyl chains. In agreement with previous studies (24), the bending angle (θ) of the polyunsaturated acyl chain showed several

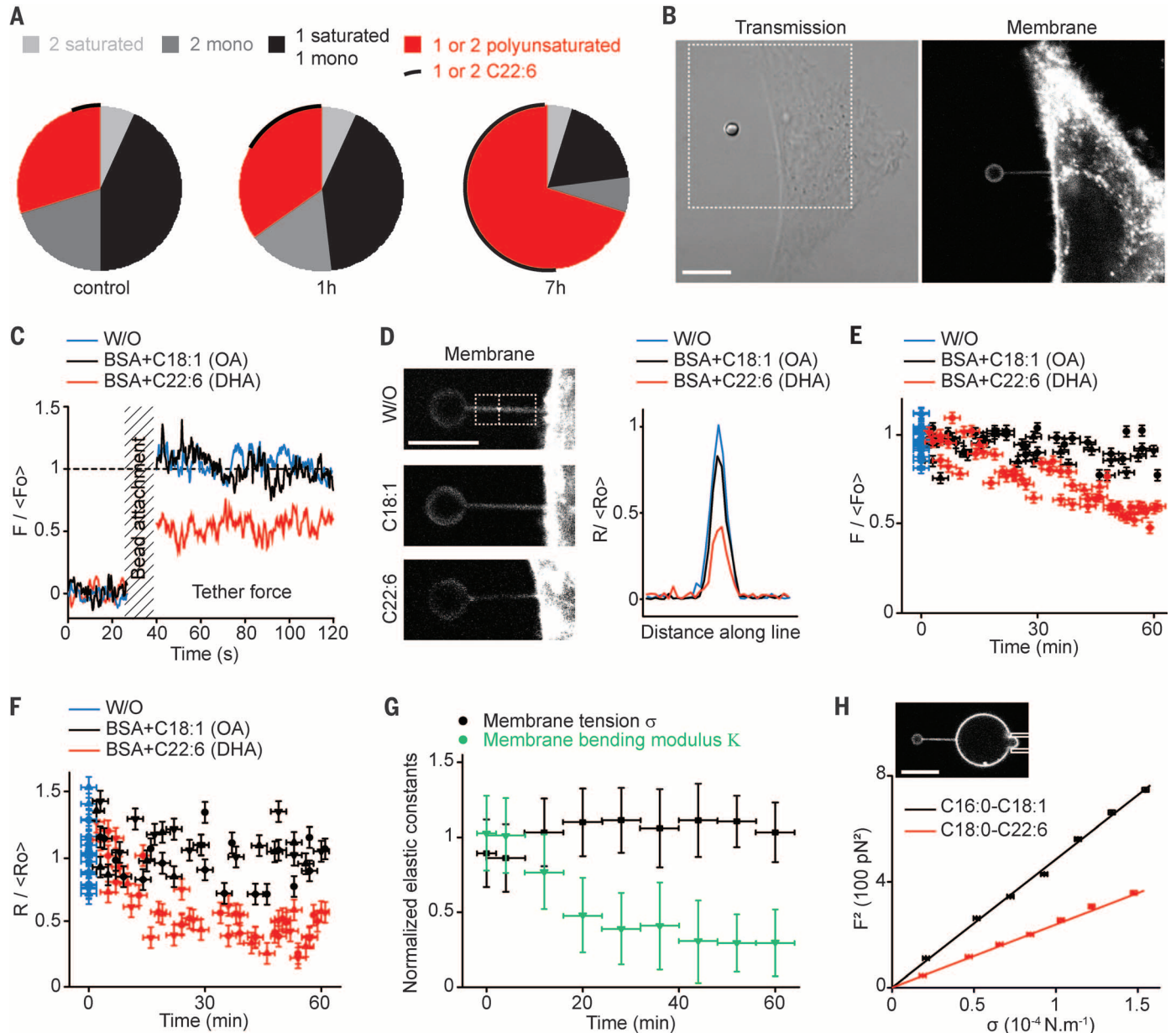


Fig. 2. Incorporation of C22:6 into cellular PLs decreases PM bending rigidity.

(A) Mass spectrometry analysis of phosphatidylcholine species in RPE1 cells after incubation with C22:6. (B) Differential interference contrast and fluorescence confocal image of a RPE1 cell plated on an L-shaped micropattern. A tube was pulled from the PM using a 3- μ m concavalin A-coated bead and an optical tweezer. Scale bar, 10 μ m. (C and D) Typical measurements of the force (F) and apparent radius (R) of cell tubes after incubation with C18:1 or C22:6 fatty acid for 1 hour. $<F_0>$ and $<R_0>$ are the mean force and mean radius, respectively, before fatty acid addition. W/O, without; OA, oleic acid; DHA,

docosahexaenoic acid. Scale bar, 5 μ m. (E and F) Evolution of F and R over time after incubation of the cell culture with C18:1 or C22:6 fatty acids (73 tubes in four independent experiments with C22:6 and 71 tubes in four independent experiments with C18:1). Error bars denote the SD of each mean. (G) Evolution of the bending modulus (κ) and tension (σ) as deduced from (E) and (F). Error bars denote the SD of each mean. (H) Tube-pulling experiments on GUVs containing 30 mol % C16:0-C18:1 PE or C18:0-C22:6 PE ($n = 7$ GUVs for each condition). A linear fit of F^2 versus σ gives $\kappa = (15 \pm 3)k_B T$ for C16:0-C18:1 PE and $(7 \pm 3)k_B T$ for C18:0-C22:6 PE (k_B , Boltzmann constant; T, temperature). Scale bar, 10 μ m.

Fig. 3. Polyunsaturated PLs stimulate Tfn endocytosis. (A) RPE1 cells overexpressing or not expressing endophilin A1 were cultured in the presence of BSA-C18:1 or BSA-C22:6 complexes for 3 hours and, when indicated, were further treated with MCD. At time = 0, fluorescent Tfn was added, and the amount of internalized Tfn at 37°C after 5 min was determined by confocal microscopy. Data were analyzed using a Student's *t* test with Welch correction; *** $P < 0.0001$ (≈ 450 cells for each condition), n.s., not significant. (B) Confocal images of total (internalized + PM) Tfn in cells incubated with C18:1 or C22:6 fatty acids and treated or not treated with MCD before endocytosis. (C) Images of internalized Tfn in C18:1- or C22:6-fed cells overexpressing endophilin A1 and, when indicated, treated with MCD before Tfn endocytosis. Colored images: single confocal planes of internalized Tfn (red) and PM (green). Black and white images: z-stacked projection of Tfn fluorescence. Scale bars (B and C), 10 μm .

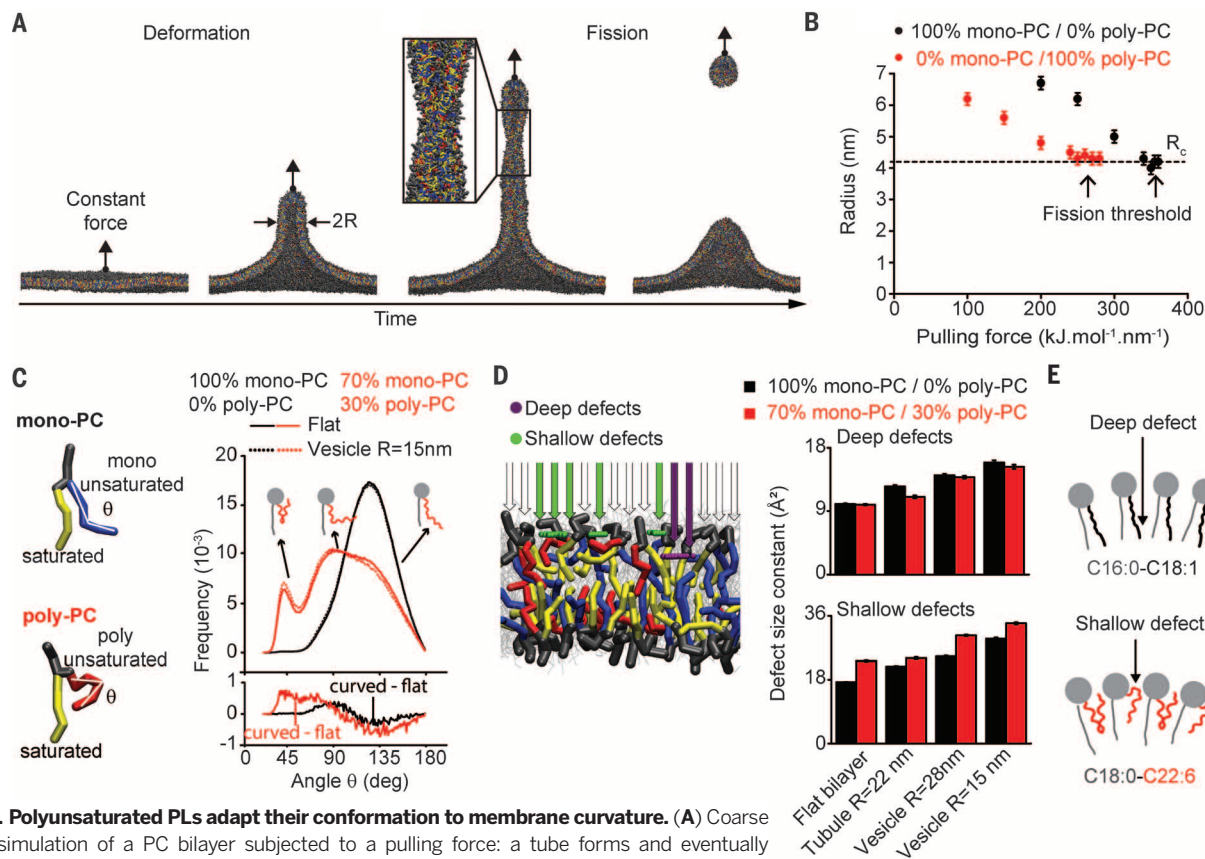
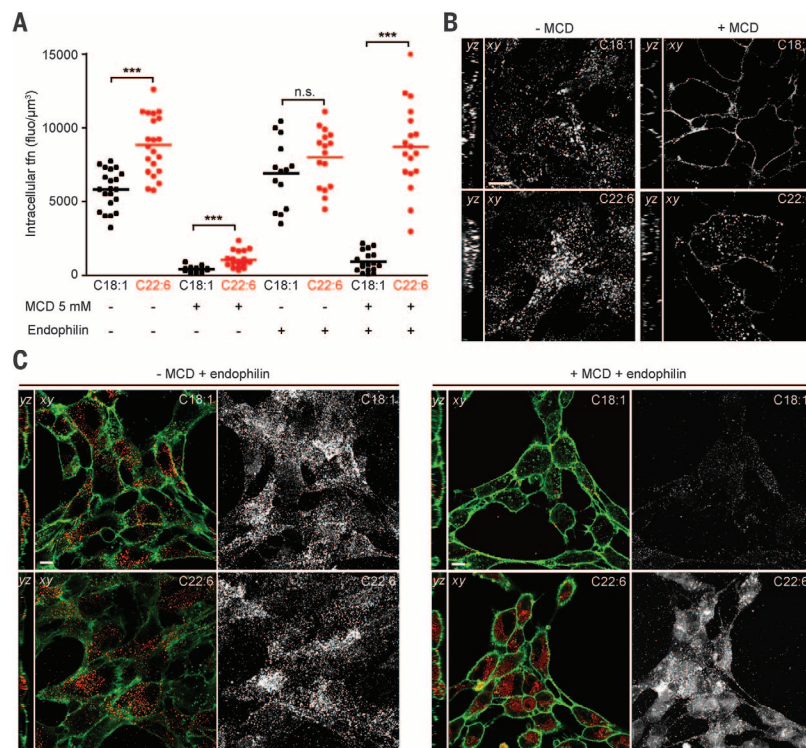


Fig. 4. Polyunsaturated PLs adapt their conformation to membrane curvature. (A) Coarse grain simulation of a PC bilayer subjected to a pulling force: a tube forms and eventually undergoes fission. R , radius. (B) Tube radius versus pulling force for bilayers containing mono or polyunsaturated PC. The dashed line indicates the critical radius for fission. Error bars indicate the SD of each mean. (C) Distribution of the bending angle (θ) of the mono- or polyunsaturated acyl chain in flat or spherical ($R = 15\text{ nm}$) bilayers. (D) Characteristic area constant of deep and shallow lipid-packing defects in bilayers of the indicated shape and containing 0 or 30 mol % polyunsaturated PC. (E) Models showing that polyunsaturated PLs adapt their conformation to membrane curvature, thereby favoring the formation of shallow lipid-packing defects at the expense of deep ones.

peaks (Fig. 4C). Positive membrane curvature shifted the angular distribution toward the kinked conformations (40° , 80°) at the expense of the more extended one (130°), whereas the angular distribution of the monounsaturated acyl chain, which peaked at $\theta = 130^\circ$, was almost unaffected (Fig. 4C).

We then looked for defects in the geometrical arrangement of lipids by scanning the surface of simulated bilayers of various shapes (Fig. 4D). A defect is a region where the first lipid atom encountered by a line normal to the surface is an aliphatic carbon (25). Using a depth threshold of 1 Å below the glycerol region (fig. S8, A and B), we observed that both deep and shallow defects increased with positive membrane curvature (Fig. 4D). However, polyunsaturated PLs promoted the formation of shallow defects and decreased the formation of deep defects, especially in curved membranes where defects were abundant (Fig. 4D and fig. S8, C and D). Thus, the angle and packing defect analyses agreed: Polyunsaturated PLs adapt their conformation to membrane curvature by using their flexible chain to fill voids in the outer monolayer (Fig. 4E).

To test this model, we took advantage of contrasting chemistries of two amphipathic helices: α -synuclein and the amphipathic lipid-packing sensor (ALPS). Both helices respond to membrane curvature, but their hydrophobic faces, which insert in the membrane, are very different (26): α -synuclein contains small residues (Val, Ala, Thr), which should be adapted to shallow defects, whereas ALPS contains bulky residues (Leu, Phe), which should be adapted to deep defects (fig. S9A). In agreement with this prediction, replacing C16:0-C18:1 PLs with C18:0-C22:6 PLs impeded the binding of ALPS to calibrated liposomes but favored the adsorption of α -synuclein (figs. S9, B to G, and S10) (27).

Polyunsaturated PLs are beneficial for health and their abundance in the brain suggests a decisive advantage for cognitive functions, but the underlying molecular mechanisms are poorly understood. By showing that polyunsaturated PLs improve the response of model membranes to the mechanical activities of endocytic proteins, our study offers a potential explanation for extraordinary speed of endocytosis in the nerve terminal (28), where polyunsaturated PLs are abundant (29). The conformational plasticity of polyunsaturated PLs may also explain their role in mechanotransduction (30).

REFERENCES AND NOTES

1. J. R. Marszalek, H. F. Lodish, *Annu. Rev. Cell Dev. Biol.* **21**, 633–657 (2005).
2. S. Takamori *et al.*, *Cell* **127**, 831–846 (2006).
3. D. C. Mitchell, S. L. Niu, B. J. Litman, *J. Biol. Chem.* **276**, 42801–42806 (2001).
4. F. Darios, B. Davletov, *Nature* **440**, 813–817 (2006).
5. A. Tixier-Vidal, R. Picart, C. Loudes, A. F. Bauman, *Neuroscience* **17**, 115–132 (1986).
6. E. Marza *et al.*, *Mol. Biol. Cell* **19**, 833–842 (2008).
7. W. Rawicz, K. C. Olbrich, T. McIntosh, D. Needham, E. Evans, *Biophys. J.* **79**, 328–339 (2000).
8. K. Farsad *et al.*, *J. Cell Biol.* **155**, 193–200 (2001).
9. A. Sundborger *et al.*, *J. Cell Sci.* **124**, 133–143 (2011).
10. Y. Yoshida *et al.*, *EMBO J.* **23**, 3483–3491 (2004).
11. J. S. Chappie, S. Acharya, M. Leonard, S. L. Schmid, F. Dydá, *Nature* **465**, 435–440 (2010).
12. M. Meinecke *et al.*, *J. Biol. Chem.* **288**, 6651–6661 (2013).
13. D. Danino, K. H. Moon, J. E. Hinshaw, *J. Struct. Biol.* **147**, 259–267 (2004).
14. A. Roux, K. Uyhazi, A. Frost, P. De Camilli, *Nature* **441**, 528–531 (2006).
15. W. Helfrich, *Z. Naturforsch. C* **28**, 693–703 (1973).
16. T. Ben Gedalya *et al.*, *Traffic* **10**, 218–234 (2009).
17. R. J. Bruckner, S. S. Mansy, A. Ricardo, L. Mahadevan, J. W. Szostak, *Biophys. J.* **97**, 3113–3122 (2009).
18. S. K. Rodal *et al.*, *Mol. Biol. Cell* **10**, 961–974 (1999).
19. A. Subtil *et al.*, *Proc. Natl. Acad. Sci. U.S.A.* **96**, 6775–6780 (1999).
20. A. McCluskey *et al.*, *Traffic* **14**, 1272–1289 (2013).
21. K. Gawrisch, N. V. Eldho, L. L. Holte, *Lipids* **38**, 445–452 (2003).

22. K. Rajamoorthi, H. I. Petrache, T. J. McIntosh, M. F. Brown, *J. Am. Chem. Soc.* **127**, 1576–1588 (2005).
23. S. Baoukina, S. J. Marrink, D. P. Tieleman, *Biophys. J.* **102**, 1866–1871 (2012).
24. H. J. Risselada, S. J. Marrink, *Phys. Chem. Chem. Phys.* **11**, 2056–2067 (2009).
25. L. Vamparys *et al.*, *Biophys. J.* **104**, 585–593 (2013).
26. I. M. Pranke *et al.*, *J. Cell Biol.* **194**, 89–103 (2011).
27. S. Kubo *et al.*, *J. Biol. Chem.* **280**, 31664–31672 (2005).
28. S. Watanabe *et al.*, *eLife* **2**, e00723 (2013).
29. H. J. Yang, Y. Sugiura, K. Ikegami, Y. Konishi, M. Setou, *J. Biol. Chem.* **287**, 5290–5300 (2012).
30. V. Vásquez, M. Krieg, D. Lockhead, M. B. Goodman, *Cell Reports* **6**, 70–80 (2014).

ACKNOWLEDGMENTS

We thank M. de Saint-Jean, C. Thonont, and F. Brau for technical help; A. Lürick for some experiments; J. B. Manneville for training and the microscope setup; J. Bigay, B. Mesmin, and A. Copic for comments on the manuscript; and all members of our laboratories for discussion. This work was supported by the CNRS, the European Research Council (advanced grant 268888), and the Agence Nationale de la Recherche (ANR) (ANR-11-LABX-0028-01). M.P. was supported by the ANR (ANR09-JCJC-0020-01) and the Fondation Pierre Gilles de Gennes. S.V. was supported by the Swiss National Science Foundation (PBELP3_141118). H.B. was supported by Inserm. Additional data described in this work can be found in the supplementary materials. Author contributions: M.P. performed experiments with GUVs; M.P. and H.B. performed mechanical experiments on cells; H.B. designed and performed endocytosis experiments; S.V. and R.G. conducted and analyzed MD simulations; L.-A.P. and T.F. performed phospholipid analysis; S.P., S.L.-G., and B.A. performed electron microscopy; B.A. designed the project, performed biochemical experiments, and wrote the manuscript with the help of B.G., S.V., H.B., and M.P.

SUPPLEMENTARY MATERIALS

www.sciencemag.org/content/345/6197/693/suppl/DC1
Materials and Methods
Figs. S1 to S10
Tables S1 to S2
References (31–49)
Movies S1 to S3

28 April 2014; accepted 14 July 2014
10.1126/science.1255288

Polyunsaturated phospholipids facilitate membrane deformation and fission by endocytic proteins

Mathieu Pinot, Stefano Vanni, Sophie Pagnotta, Sandra Lacas-Gervais, Laurie-Anne Payet, Thierry Ferreira, Romain Gautier, Bruno Goud, Bruno Antony, and H el ene Barelli

Science, 345 (6197), • DOI: 10.1126/science.1255288

Bending the benefits of polyunsaturates

We have often heard that it is beneficial to eat polyunsaturated fatty acids. We also know that some organelles such as synaptic vesicles are extremely rich in polyunsaturated lipids. However, what polyunsaturated lipids do in our body is unclear. Using cell biology, biochemical reconstitutions, and molecular dynamics, Pinot *et al.* show that polyunsaturated phospholipids can change the response of membranes to proteins involved in membrane curvature sensing, membrane shaping, and membrane fission. Polyunsaturated phospholipids make the plasma membrane more amenable to deformation; facilitate endocytosis; and, in reconstitution experiments, increased membrane fission by the dynamin-endophilin complex.

Science, this issue p. 693

View the article online

<https://www.science.org/doi/10.1126/science.1255288>

Permissions

<https://www.science.org/help/reprints-and-permissions>

Use of this article is subject to the [Terms of service](#)